Icarus **158**, 281–293 (2002)
doi:10.1006/icar.2002.6895

The Nebular Shock Wave Model for Chondrule Formation: Shock Processing in a Particle–Gas Suspension

Fred J. Ciesla and Lon L. Hood

Lunar and Planetary Laboratory, University of Arizona, 1629 E. University Boulevard, Tucson, Arizona 85721
E-mail: fciesla@lpl.arizona.edu

Received April 5, 2001; revised April 9, 2002

We present numerical simulations of the thermal and dynamical histories of solid particles (chondrules and their precursors—treated as 1-mm silicate spheres) during passage of an adiabatic shock wave through a particle–gas suspension in a minimum-mass solar nebula. The steady-state equations of energy, momentum, and mass conservation are derived and integrated for both solids and gas under a variety of shock conditions and particle number densities using the free-molecular-flow approximation. These simulations allow us to investigate both the heating and cooling of particles in a shock wave and to compare the time and distance scales associated with their processing to those expected for natural chondrules. The interactions with the particles cause the gas to achieve higher temperatures and pressures both upstream and downstream of the shock than would be reached otherwise. The cooling rates of the particles are found to be nonlinear but agree approximately with the cooling rates inferred for chondrules by laboratory simulations. The initial concentration of solids upstream of the shock controls the cooling rates and the distances over which they are processed: Lower concentrations cool more slowly and over longer distances. These simulations are consistent with the hypothesis that large-scale shocks, e.g., those due to density waves or gravitational instabilities, were the dominant mechanism for chondrule formation in the nebula.

Key Words: **meteorites; Solar System origin; solar nebula; thermal histories.**

1. INTRODUCTION

Chondritic meteorites have as significant components (up to 80% by volume) chondrules—roughly millimeter-sized, once molten, silicate particles. Chondrules are believed to have formed in the solar nebula (e.g., Hewins 1997), therefore, understanding the processes that controlled chondrule formation should provide insight into the early evolution of our Solar System. To fully understand how chondrules formed, one must identify how their precursors melted on timescales of seconds to minutes, cooled at rates of 10–1000 K h^{-1}, accreted fine-grained rims composed of material similar to the chondrules themselves, were processed more than once, and were then incorporated into planetesimals.

Currently, gas dynamic shock waves in a relatively cool (<650 K) protoplanetary nebula are considered likely environments for chondrule formation (for reviews, see Boss 1996, Hewins 1997, Connolly and Love 1998). Shocks with velocities around 6–7 km/s near the midplane of a nominal low-mass nebula containing 0.1–1.0-mm-sized precursor aggregates are capable of thermally processing these grains to melting temperatures consistent with meteoritic data (Wood 1984, Hood and Horanyi 1991, 1993, Ruzmaikina and Ip 1994, Desch and Connolly 2002). Shock waves are also capable of sorting particles in the nebula by size and forming dusty, volatile-rich rims around chondrules (e.g., Connolly and Love 1998). Possible energy sources of gas dynamic shocks near the nebula midplane include spiral density waves in a gravitationally unstable nebula (Wood 1996, Boss 2000) and planetesimals scattered gravitationally into eccentric/inclined orbits by a protoJupiter (Hood 1998, Weidenschilling *et al*. 1998).

A basic one-dimensional (1-D) physical model for the formation of chondrules during the passage of gas dynamic shock waves through the solar nebula has been developed (Hood and Horanyi 1991, 1993) (hereafter referred to as HH91 and HH93). HH91 described the equations that governed gas–chondrule interactions in a shock. However, they only considered the processing of a single precursor. Observations of the collision history and the inferred composition of the gas in which chondrules formed imply that chondrules may have formed in zones enriched in solids over the canonical solar value (total solids-to-gas mass ratios up to 1000 times solar). Although some aspects of the interaction of shocked gas with a cloud of particles (rather than a single particle) were treated by HH93, a more accurate treatment should consider the general problem of a shock wave passing through a particle–gas suspension (e.g., Igra and Ben-Dor 1980). As a shock front passes through a particle-rich zone, the resulting interactions increase the gas temperature, density, and pressure with distance behind the shock relative to that which would exist in the absence of any solids. These changes in gas properties lead to very different processing histories of the particles than are obtained in the single particle limit. For a given set of nebula and particle parameters, a smaller shock velocity may therefore be required for precursor particle melting in

0019-1035/02 $35.00

solids-rich zones. While HH93 did consider the exchange of radiation between chondrules, the method for calculating the energy transfer was a first-order approximation and considered the radiation from a finite volume around the chondrules. A better treatment which uses the principles of radiative transfer and calculates the radiative contribution from all chondrules is needed. In addition, HH91/93 focused mainly on melting of the chondrules, i.e., on the first few seconds or minutes during which they were processed. Laboratory analyses have been able to constrain the evolution of chondrules over timescales of hours. A detailed treatment of the evolution of the particle–gas suspension behind the shock front that quantitatively investigates the cooling of the particles will allow for a better evaluation of the shock model for chondrule formation based on these constraints.

In this paper, we extend the HH91/93 model to account more completely for the effects of energy and momentum transfer between the particles and gas, including a more rigorous treatment of radiative energy transfer between particles than that used in HH93. In Section 2, we discuss several different lines of evidence suggesting that the chondrule-forming environment was enriched in solid particles over the canonical solar value and we review possible ways in which these enhancements come about. In Section 3, a steady-state model appropriate for a shock wave passing through an infinite particle–gas suspension under conditions similar to those of the solar nebula is presented. The results from integration of the model equations are given in Section 4 for a range of different shock velocities and particle densities. The implications of this work and suggestions for future work are discussed in Section 5.

2. ENHANCEMENTS OF SOLIDS IN THE SOLAR NEBULA

The belief that the chondrule-forming region in the solar nebula was enriched in solids is supported by three main findings: (1) the inferred oxygen fugacity of the chondrule-formation region (Wood 1985, Kring 1988, Lauretta *et al*. 2001), (2) the presence of fine-grained rims on chondrules (Kring 1988, Connolly and Love 1998, Liffman and Toscano 2000), and (3) the collisional history of chondrules (Gooding and Keil 1981, Lofgren and Hanson 1997). Each of these lines of evidence warrants some discussion (for more discussion, see also Hood and Ciesla 2001).

The large fayalite content in the olivine of some chondrules has led many authors to conclude that the oxygen fugacity regions of the nebula where chondrules formed may have been up to 1000 times the solar value (Wood 1985, Kring 1988). In addition to oxygen fugacities, the enhancement of other solid-forming elements helps to explain the petrology of chondrule-derived metal and its corrosion products (Lauretta *et al*. 2001). Lauretta *et al*. (2001) calculated that the metals in their samples reacted with a nebular gas that had an atomic dust/gas ratio of ∼350. Finally, Ozawa and Nagahara (1997) demonstrated that evaporation of chondrule melts is suppressed only in a nebula gas enriched in dust-forming species by many orders of magnitude. The favored way of achieving such values is through the vaporization of dust (∼1 micron) particles during the flash heating of the chondrules. Some authors (e.g., Huang *et al*. 1996) have proposed that some of these same observations can be explained by different intensities of heating rather than by different environmental conditions, though they do concede that the environmental conditions may still be important.

Fine-grained rims (dust mantles) are found around chondrules in most unequilibrated chondrites. Connolly and Love (1998) proposed that these rims could be explained by the collision of chondrules with a mixture of gas and small-scale dust. Liffman and Toscano (2000) demonstrated that this was possible if the dust-to-gas mass ratio was roughly 0.5 to 1.0 (100–200 times the solar value) and if dust–chondrule sticking coefficients were in the range of 0.5 to 1.0.

Finally, the presence of compound and cratered chondrules demonstrates that chondrules experienced collisions at a time when they were "plastic" or partially molten. Gooding and Keil (1981) compiled statistics for over 1600 chondrules and found that the "chondrule population value" (the probability that two chondrules would collide to produce a compound or cratered chondrule) was in the range of 2–14%. Following their derivations, one can calculate the chondrule number density based upon the chondrule population value, P. The number density is found from

$$n_c = P(\sqrt{2}\pi D^2 \bar{v} t)^{-1}, \quad (1)$$

where D is the chondrule diameter, $\bar{v}$ is the average collisional speed of each chondrule, and t is the time that a chondrule is "plastic" or deformable. Setting D to 0.1 cm, and adopting values from Gooding and Keil (1981) ($\bar{v} \sim 10^4$ cm s^{-1} and $t \sim 10$–100 s), one finds typical values of $n_c > 0.5$–3 m^{-3}.

As noted by Gooding and Keil (1981), the values of the above parameters have significant uncertainties. The value of $\bar{v}$ that they use, 10^4 cm s^{-1}, is an assumed upper limit. Kring (1991) estimated that the relative velocities at which molten droplets could collide and survive were $\leq$130 cm s^{-1}. In addition, Weidenschilling (1988) argued that 100 cm s^{-1} was a typical velocity that would prevent collisional destruction. Using $\bar{v} \sim 100$ cm s^{-1}, one finds $n_c > 50$–300 m^{-3}. However, given that chondrules cooled at rates between 10 and 1000 K h^{-1}, and assuming that chondrules remained deformable for a temperature interval of order 100 K, then a better value for t would be approximately 1 h ($\sim 10^3$ s). This lowers the estimate for n_c to $>$5–30 m^{-3}. It is worth noting that these calculations were done for $D = 0.1$ cm, which is roughly an upper limit on the size of chondrules. Chondrules can have diameters as small as 0.01 cm, which would increase n_c by a factor of 100. Considering all uncertainties, we consider $n_c \sim 1$–10 m^{-3} (dust–gas mass ratio 30–300 times solar in a minimum mass nebula) to be a valid estimate. Other methods have been suggested for producing compound chondrules (Wasson *et al*. 1995), but further support has also been given in favor of the low-velocity collision model (Lofgren and Hanson 1997).

The idea that the chondrule-forming environment was one in which solids had been concentrated has led many to conclude that chondrules were formed at the midplane of the nebula, where solids settled gravitationally (e.g., Radomsky and Hewins 1990). However, it has been argued that such settling of small particles to the midplane would be inhibited by the expected turbulent nature of the nebula (Weidenschilling 1984, Cuzzi *et al.* 1996, 2001). The latter authors argue that particles with similar sizes and densities as chondrules could be concentrated above the midplane in turbulent eddies. The concentration of solids in their simulations reached typical values of 40–300 times the solar solids-to-gas mass ratio and in some cases could be as high as 10^5 times solar (Cuzzi *et al.* 2001). This mechanism was most effective for concentrating chondrule-size particles and was not effective at concentrating fine dust.

Several other mechanisms for locally enhancing the amount of solids in parts of the nebula exist beyond turbulent concentration. If shock waves existed in the nebula due to supersonic planetesimals, as proposed by Hood (1998) and Weidenschilling *et al.* (1998), collisions between planetesimals are likely to have occurred. These collisions would have produced dust which could have led to dust enhancements, particularly near orbital resonances with a protoJupiter. Also, if large bodies existed, such as a protoJupiter, formed either by core accretion (e.g., Weidenschilling *et al.* 1998), or by gravitational instabilities (Boss 2000), in the nebula, there would have been gravitational and centrifugal equilibrium points (such as the Lagrange points) where dust would have been preferentially concentrated. If many massive bodies existed in the early solar nebula, as is expected, there would be many points where dust could have been locally enhanced by dynamical means. Finally, as explored in this paper, nebular shocks themselves may represent an additional mechanism for spatially concentrating particles.

In conclusion, although there are various interpretations of the data, several different lines of evidence suggest that the environment in which chondrules formed was one in which solids were highly concentrated, at least initially. In the next section, we develop a model that treats the passage of a shock through a suspension of nebular gas and chondrule precursors of arbitrary number density. Although the possible additional presence of small-scale dust is not treated (cf. Hood and Ciesla 2001), the model represents a useful step toward accounting for the effects of multiple particles in the chondrule-formation region.

3. THE MODEL

The effects of a shock passing through a particle–gas suspension have been studied in some detail by Igra and Ben-Dor (1980). In their model, they consider a suspension initially in thermal and kinetic equilibrium (the particles and gas are at the same temperature and there is no relative velocity between the two species). Upon passage through the shock front, the temperature, velocity, and density of the gas change in a way given by the Rankine–Hugoniot relations. The particles, however, pass through the shock front unaffected. Immediately behind the shock front, there is a state of disequilibrium between high-temperature–low-velocity (with respect to the shock front) gas and low-temperature–high-velocity particles. Over some distance, termed the "relaxation zone," energy and momentum are exchanged between the two species until a new state of equilibrium is established. Due to these exchanges, the temperature of the gas is increased due to the loss of the particle kinetic energy. This feedback led to a correlation between temperatures and pressures and dust concentrations.

Igra and Ben-Dor (1980) considered only the case for shocks in the lower terrestrial atmosphere, that is, at gas densities many orders of magnitude greater than expected for the solar nebula. In addition, these authors did not allow for phase transitions of the particles in the suspension, nor did they account for the exchange of radiation between the particles. Therefore, in order to formulate a model similar to that of Igra and Ben-Dor (1980), several modifications are necessary.

First, at the lower shocked gas number densities ($<3 \times 10^{16}$ cm^{-3}) appropriate for the solar nebula, the free molecular flow limit (mean free path much greater than dust particle size) is valid. Gas–particle energy transfer rates can therefore be calculated using analytic expressions that depend on the gas–particle relative velocity and the temperatures of the particles and the gas (e.g., Gombosi *et al.* 1986, HH91). Secondly, because Igra and Ben-Dor (1980) considered a higher density gas, the length of the relaxation zone was only on the order of a few meters. In this study, the distance over which equilibrium between the chondrules and gas is achieved can be on the order of thousands of kilometers. This requires consideration of how radiation is exchanged between the particles. While this was addressed in HH93, we present a more rigorous calculation that does not make any assumptions about the temperatures of the particles but rather calculates a radiation flux based on the actual temperature profile. This includes the warming of the particles upstream from the shock. Thirdly, we have allowed for the possibility of latent heat absorption or release as the particles are melted, vaporized, or crystallized.

In order to formulate a model for the thermal and dynamical evolution of a particle–gas suspension during passage of an adiabatic shock wave that can be applied to chondrule formation, we first follow Igra and Ben-Dor (1980) in adopting a series of simplifying assumptions:

1. Solids are present in the suspension only as chondrules or chondrule precursors, i.e., no micron-sized dust is present (precursor refers to the solids upstream from the shock front, chondrule refers to those downstream of the shock, and particle refers to both).

2. The particles are rigid, chemically inert, identical spheres distributed uniformly throughout the gas.

3. Particles do not physically interact with each other except for the exchange of radiative energy, and the total particle volume is negligible compared to the gas volume.

4. At large distances ahead of the shock, the chondrule precursors are in a state of thermal and dynamical equilibrium with the gas.

5. The temperature within each particle is uniform.

6. Particle weight and buoyancy forces are negligible, and the particles are too large to experience Brownian motion in the gas.

7. The gas properties change across the shock front in a way given by

$$\frac{T_2}{T_1} = \frac{[2\gamma M^2 - (\gamma - 1)][(\gamma - 1)M^2 + 2]}{[(\gamma + 1)^2 M^2]} \tag{2}$$

$$\frac{n_2}{n_1} = \frac{(\gamma + 1)M^2}{[(\gamma - 1)M^2 + 2]} \tag{3}$$

$$\frac{v_2}{v_1} = \frac{n_1}{n_2}, \tag{4}$$

where T, n, and v represent the gas temperature, number density, and velocity with respect to the shock front, the subscripts 1 and 2 represent the values immediately before and after the shock, respectively, and M is the ratio of the speed of the gas with respect to the shock front to the speed of sound in that gas immediately before passage through the front.

For the above assumptions, the steady-state equations of mass, momentum, and energy conservation, in a frame of reference moving with the shock front, may be written in the form

$$\frac{d}{dx}(\rho_g v_g) = 0 \tag{5}$$

$$\frac{d}{dx}(\rho_c v_c) = 0 \tag{6}$$

$$\frac{d}{dx}\left(\rho_g v_g^2\right) + \frac{dP}{dx} = -F_D \tag{7}$$

$$\frac{d}{dx}\left(\rho_c v_c^2\right) = F_D \tag{8}$$

$$\frac{d}{dx}\left[\left(C_v T_g + \frac{1}{2}v_g^2\right)\rho_g v_g + P v_g\right] = -Q_{gc} - F_D v_c \tag{9}$$

$$\frac{d}{dx}\left[\left(C_c T_c + \frac{1}{2}v_c^2\right)\rho_c v_c\right] = Q_{gc} + Q_{cc} - Q_{cr} + F_D v_c, \tag{10}$$

where x is the one-dimensional spatial coordinate, ρ_g and ρ_c are the respective mass densities of gas and particles in the suspension, v_g and v_c are the corresponding velocities with respect to the shock front, T_g and T_c are the corresponding temperatures, C_v and C_c are the corresponding specific heats (at constant volume for the gas), P is gas pressure, F_D is the drag force per unit volume acting on the particles, Q_{gc} is the rate of energy transfer from the gas to the particles per unit volume due to gas drag and thermal collisions, Q_{cc} is the rate of radiative energy transfer to particles from other particles per unit volume, and Q_{cr} is the rate of energy loss by radiation from the particles per unit volume. In (10), the last terms on the right-hand side represents the effect of gas drag on the rate of particle kinetic energy density change in a frame of reference moving with the shock front. In (9), an equal and opposite term is on the right-hand side to account for the effect on the gas.

In (7)–(10), the drag force per unit volume is expressed as

$$F_D = -\frac{1}{2}\rho_g(v_c - v_g)|v_c - v_g|C_D\frac{\pi}{4}D^2 n_c, \tag{11}$$

where D is the particle diameter, n_c is the particle number density, and C_D is the drag coefficient. For the special case of perfectly elastic collisions of gas molecules and particles, the drag coefficient $C_D \simeq 2$ (e.g., Whipple 1950). For more realistic conditions, C_D depends on the temperature of the gas and the relative velocity of the particles with respect to the gas (see equation (3) of HH91).

As noted above, we adopt here the free molecular flow approximation, which is valid for millimeter-sized particles in a hydrogen-dominated gas provided that the number density of gas molecules is less than about 3×10^{16} cm^{-3} (HH91). In this approximation, the rate of thermal energy transfer from the gas to the particles per unit volume is given by

$$Q_{gc} = \pi D^2 n_c \rho_g |v_c - v_g|(T_{rec} - T_c)C_H, \tag{12}$$

where T_{rec} is the adiabatic "recovery" temperature (defined as the particle temperature at which thermal heat transfer is zero) and C_H is the heat transfer function or Stanton number. Detailed expressions for these terms can be found in Gombosi *et al.* (1986) and HH91.

As discussed above, previous treatments of radiation exchange among the chondrules by HH93 considered only exchange of radiation between chondrules in a relatively small volume. A more correct treatment in this model would use principles of radiative transfer (Desch and Connolly 2002) to find Q_{cc} and Q_{cr}. This topic has been addressed in detail by many authors (e.g., Mihalas 1970, Ozisik 1977, Collison and Fix 1991, and Tanaka *et al.* 1998). For the purposes of this paper, we ignore all effects in the radiative transfer that are dependent on the frequency of the radiation and consider the typical "gray" case.

The equation of transfer in this case is

$$\mu\frac{dI}{d\tau} = I - S, \tag{13}$$

where I is defined as the specific intensity of the radiation at a given point in space, τ is a measure of optical depth into the suspension, S is the source function of the radiation from the particles, and μ is equal to $\cos\theta$ where θ is the angle between the direction the radiation is traveling and the normal to the surface that we are considering. The equation of transfer has a

solution (Mihalas 1970):

$$I(\tau_1, \mu) = I(\tau_2, \mu)e^{-\frac{(\tau_2-\tau_1)}{\mu}} + I(0, \mu)e^{-\frac{\tau_1}{\mu}} + \int_{\tau_1}^{\tau_2} S(t)e^{-\frac{t-\tau_1}{\mu}}\frac{dt}{\mu} + \int_0^{\tau_1} S(t)e^{-\frac{\tau_1-t}{\mu}}\frac{dt}{\mu}. \quad (14)$$

Here, τ_1 represents the optical depth at which we are calculating the specific intensity, and τ_2 is the optical depth at the end of the region we are considering. Following Tanaka *et al.* (1998), we consider only silicates (i.e., the chondrules) as the opacity source, and thus we set the source function equal to the Planck function and integrate over all frequencies to find $I(\tau_1, \mu)$. In the case of a one-dimensional shock as we are considering, we integrate over all μ to find the specific intensity at the proper optical depth, or $\bar{I}(\tau_1)$.

Using (14), the specific intensity can be found at any point in the suspension, provided the temperature is known everywhere. At large distances in front of the shock, the chondrule precursors are assumed to be at the same temperature as the gas, and this dictates the first boundary condition. The second boundary condition makes the same assumption that the chondrules very far behind the shock are at a constant temperature equal to the initial temperature of the suspension; the exact position at which this temperature is reestablished is found by the integrations. For the particles closer to the shock front, the temperature profile will vary with position. In this case, the integrations are calculated numerically.

Once I is known at a given position, the amount of radiative energy absorbed by the particles per unit volume per unit time can be found using equation (1–18) of Mihalas (1970):

$$dE = \kappa\ I\ d\omega\ dt\ \rho\ dA\ ds. \quad (15)$$

This equation gives the amount of energy absorbed, dE, from a beam passing through a volume of cross section dA and length ds per time dt. The $d\omega$ represents the infinitesimal solid angle that the beam originates from and can be written $\sin\theta\, d\theta\, d\phi$. Using our definition from above for μ, we can write, for an azimuthally symmetric case:

$$d\omega = 2\pi\ d\mu. \quad (16)$$

We wish to define Q_{cc}, which is the amount of energy absorbed per unit volume per unit time, thus:

$$Q_{cc} = \frac{dE}{dA\, ds\, dt}. \quad (17)$$

This requires knowing the absorption coefficient, κ, for the particles, given by

$$\kappa = \frac{\pi D^2 \varepsilon_{abs}}{4m_c}, \quad (18)$$

where ε_{abs} is the frequency-averaged absorptivity of the particles and m_c is the mass of a particle. This gives

$$Q_{cc} = \int \rho_c \kappa \bar{I}(\tau)\, d\omega. \quad (19)$$

Similarly, the amount of energy added to a beam of radiation is given by (Mihalas 1970)

$$dE = j\ d\omega\ dt\ \rho\ dA\ ds. \quad (20)$$

This allows us to define

$$Q_{cr} = \int j\ \rho\ d\omega. \quad (21)$$

If we assume that the particles are in equilibrium with the radiation field, then

$$j = \kappa \int_0^\infty B_\nu(T)\, d\nu, \quad (22)$$

where $B_\nu(T)$ is the Planck function. Thus,

$$Q_{cr} = 4\rho\kappa\sigma T^4. \quad (23)$$

Because the radiation calculations require knowledge of the temperature of the particles throughout the suspension, we first find the temperature of the chondrules after they pass through the shock front based on the other modes of heat transfer. The particles are then sent through the shock again, and the heat transferred due to radiation from the other particles is calculated using the temperature profile as a function of distance. The procedure is iterated until the specific intensity does not change by more than 1%.

The gas is considered to be ideal in this model; that is, effects such as the dissociation of hydrogen have been ignored. In addition, radiative cooling due to rotational and vibrational transitions of molecules has been neglected. While these processes have been studied by previous authors (Ruzmaikina and Ip 1994, Iida *et al.* 2001), in the future they should be considered in the context of a particle–gas suspension. Preliminary studies by Ciesla and Hood (2000) found that hydrogen dissociation acts as an energy sink, requiring a larger shock velocity for the formation of chondrules than that required in cases where dissociation is ignored. Desch and Connolly (2002) also found that dissociation led to lower peak temperatures of chondrules than those that occur in the absence of this effect.

4. MODEL RESULTS

A FORTRAN program was written to numerically integrate the above equations using a Runge–Kutta adaptive step-size method. For the cases studied in this paper, the following values were adopted (same as Hood 1998): a gas specific heat ratio of

7/5, a gas mean molecular mass of 4×10^{-24} g, a particle specific heat of 10^7 erg g^{-1} K^{-1}, a particle latent heat of melting of 4.5×10^9 erg g^{-1}, a melting temperature of 1900 K (where all the latent heat of melting is gained), a vaporization temperature of 2100 K (though we will not present any runs where the chondrules begin to vaporize), and particle diameters of 0.1 cm. The particle wavelength-averaged emissivities and absorptivities were assumed to be 0.9 following HH93. The particle mass density was considered to be 3.0 g cm^{-3}. In all of the simulations reported here, the ambient nebula is assumed to be at a temperature of 400 K with a gas mass density upstream of the shock equal to 1×10^{-9} g cm^{-3} which gives a pressure of 1.4×10^{-5} atm (roughly appropriate for the asteroid belt region in a minimum mass nebula).

4.1. Case 1: $n_c = 1$ m^{-3}, $V_s = 7.6$ km s^{-1}

We first investigate the case of a shock passing through such a nebula with a chondrule precursor number density of 1 m^{-3} (solids-to-gas mass density ratio of ∼1.5, or roughly 300 times solar) far upstream of the shock. Figure 1 shows the temperature of the particles in the suspension as a function of time, with the chondrule precursors passing through the shock front at $t = 0$. The velocity of the shock was chosen to be 7.6 km s^{-1} with respect to the upstream gas. This velocity is just sufficient to completely melt the chondrules without vaporization.

Four distinct zones can be identified in the shock processing of a particle–gas suspension. The first zone is at a large distance upstream from the shock where the chondrule precursors are in a state of equilibrium with the gas (same temperature and no relative velocity). The second zone is the warming zone immediately upstream from the shock where the precursors are warmed by radiation from behind the shock. The third zone begins at the shock front when the precursors pass through unaffected but the gas properties change dramatically. This zone is where energy and momentum are exchanged between the chondrules and gas, and it lasts until a new state of equilibrium is reached. This is the relaxation zone studied by Igra and Ben-Dor (1980). Finally, the fourth zone begins at some distance significantly downstream from the shock front where the chondrules and gas remain in a state of equilibrium with different densities than in the first zone. The last three zones are shown in Fig. 1.

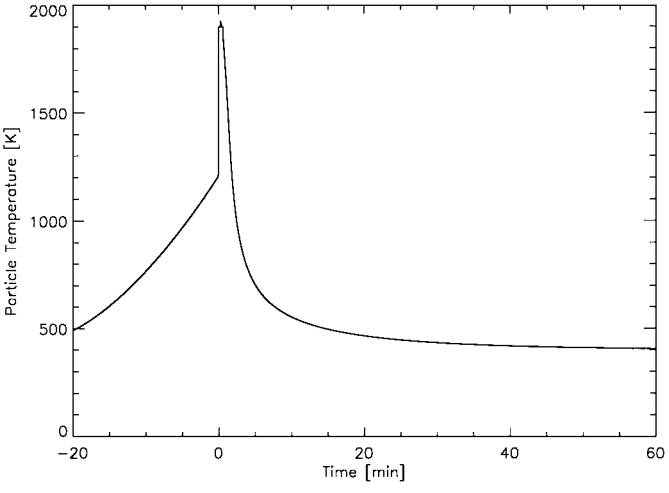

FIG. 1. The temperature of shock-processed chondrule precursors with a diameter of 0.1 cm initially suspended at a number density of 1 m^{-3} in a nebula at 400 K with a gas density of 1×10^{-9} g cm^{-3}. The shock velocity with respect to the distant upstream gas is 7.6 km s^{-1}.

Precursors are significantly warmed prior to passing through the shock front in the case considered. Immediately behind the shock front, the chondrule temperature quickly rises to the melting point and they begin to melt 3 s after crossing the shock front. The chondrules are completely melted after 15 s, when their temperature continues to rise to a peak of 1924 K at 17 s. At this point, the relative velocity between the chondrules and the gas has decreased sufficiently so that the heating rate of the chondrules (due to both gas drag and radiation from other chondrules) is less than the radiative cooling rate, and the temperature decreases. The chondrules are fully crystallized again 38 s after crossing the shock front. They then continue to cool to the equilibrium temperature of 400 K roughly 1 h after passing through the shock.

After reaching their peak temperature, the chondrules cool a total of ∼1500 K in a 1-h period. However, the cooling rate during the time period immediately after melting is much greater. If we consider the instantaneous cooling rate when the chondrules are at 1500 K (a lower temperature when most chondrules are assumed to be partially molten), the cooling rate is found to be roughly 24,000 K h^{-1}, which is over an order of magnitude greater than the experimentally inferred cooling rates (e.g., Radomsky and Hewins 1990). As the chondrules cool, they help to cool the gas as well. The gas will transfer energy to the chondrules through thermal collisions (once the relative velocity is small), and the chondrules then radiate away that energy. A higher concentration of chondrules provides more available surface area for this transfer to take place, allowing the system to cool more quickly.

Figure 2 shows the number density of the chondrules as a function of time. Immediately behind the shock, the number density increases most dramatically, increasing by a factor of 80 in the 10 min after passing through the shock, resulting in a density of over 100 m^{-3} after 1 h. This is a much higher value than that expected from the Gooding and Keil (1981) studies. It is therefore likely that a lower initial density of chondrule precursors will become concentrated to values inferred above based on the collisional histories after passing through the shock. By comparing Figs. 1 and 2, it can be seen that the temperature of the chondrules is linked to their density in the suspension. Because the density of the chondrules increases by over two orders of magnitude behind the shock, one optical depth corresponds to a much smaller spatial distance. Since the chondrules initially have a large velocity, they pass through many optical depths very quickly and thus are effectively shielded from the radiation of the warm particles immediately behind the shock. The cooling

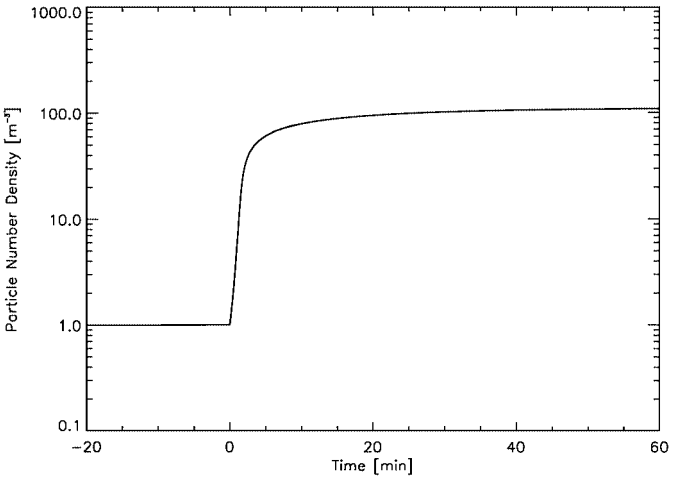

FIG. 2. The number density of chondrule precursors as a function of time for the shocked suspension of Fig. 1.

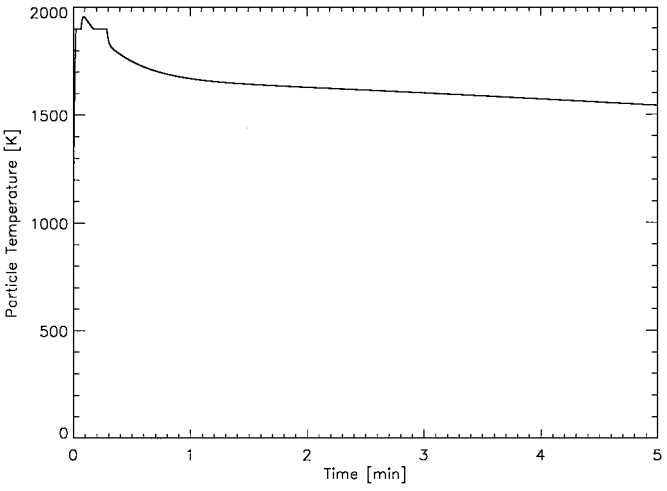

FIG. 4. The temperature profile of the same chondrules shown in Fig. 3 but for only the first 5 min behind the shock.

of the suspension is controlled mainly by energy transfer from the shock-heated gas to the solids, which in turn lose energy by thermal radiation. A lower concentration of particles would lessen these effects as well. Thus, in this model, an inital particle density of 1 m^{-3} is too great to produce chondrules.

4.2. Case 2: $n_c = 0.1\ m^{-3}$ and $V_s = 8.5\ km\ s^{-1}$

Figure 3 shows the particle temperature profile for chondrule precursors initially suspended in the nebula at a density of 0.1 m^{-3} (30 times the solar abundance of silicates). The shock speed selected for this case is 8.5 km s^{-1}. In zone 2, the chondrule precursors are warmed over a longer period of time (∼3.5 h) than in the previous case due to the decrease in optical thickness of the suspension upstream from the shock, reaching a temperature of 1054 K before passing through the shock front. The particles

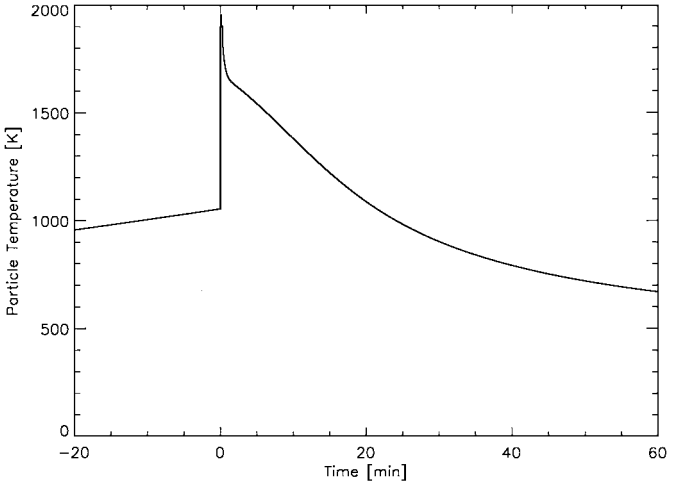

FIG. 3. The temperature of shock-processed chondrule precursors initially suspended at a number density of 0.1 m^{-3} in a nebula with the same temperature and mass density as that of Fig. 1. The velocity of the shock was 8.5 km s^{-1} with respect to the distant upstream gas.

begin melting about 1.5 s after crossing the shock front and are completely melted after 4 s. They reach a peak temperature of 1956 K after 5.5 s and then begin to cool. They are fully crystallized 10.4 s after crossing the shock front. It is interesting to note that while in the previous case the chondrules returned to their original temperature of 400 K nearly 1 h after passing through the shock front, in this case it takes over 30 h for the chondrules to cool back to exactly 400 K. Focusing on the time immediately after melting, as shown in Fig. 4, it is seen that the chondrules cool very rapidly for about 1 min before reaching a more gradual cooling rate. Considering the average cooling rate during the time interval beginning when the chondrules are at their peak temperature and ending when they reach a temperature of 1500 K, the cooling rate is found to be ∼4000 K h^{-1}. However, the cooling rate is much more gradual from 1 to 5 min after passing through the shock (an interval in which the chondrules are still above the molten limit of ∼1500 K). Over this period, the cooling rate is roughly 1800 K h^{-1}, only slightly larger than experimentally inferred chondrule cooling rates.

Figure 5 shows the number density of the particles in the same simulation. The chondrules are above our assumed "plastic" temperature of 1500 K for 6 min after reaching their peak temperature. In that time, the number density of the chondrules rises to slightly greater than 0.8 m^{-3}. Using Eq. (1), setting $t = 360$ s, and keeping $\bar{v} = 100$ cm s^{-1} and $D = 0.1$ cm, we find that 0.08% of the chondrules should be compound or cratered. This is two orders of magnitude below the estimates of Gooding and Keil (1981). Since this simulation produced cooling rates similar to those on the high end expected for chondrules, we next investigate a case for a lower initial particle density.

4.3. Case 3: $n_c = 0.003\ m^{-3}$ and $V_s = 8.5\ km\ s^{-1}$

Figure 6 shows the particle temperature profile for a suspension with a solar solids-to-gas ratio (∼0.003 chondrules m^{-3}). The chondrule precursors are warmed for over 100 h, reaching

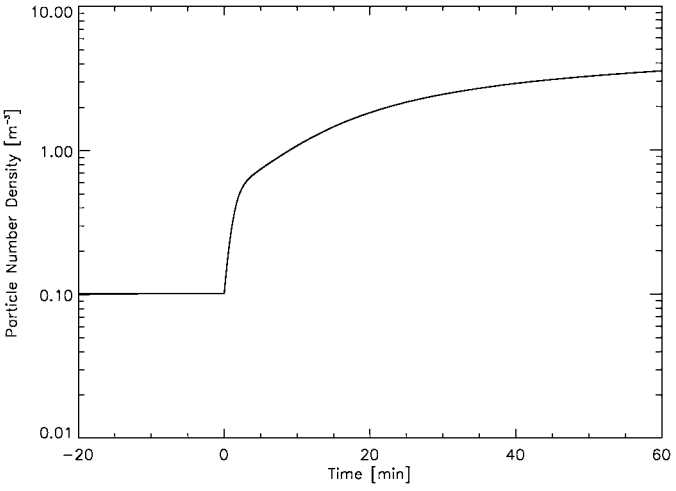

FIG. 5. The number density of chondrule precursors as a function of time for the shocked suspension described in Figs. 3 and 4.

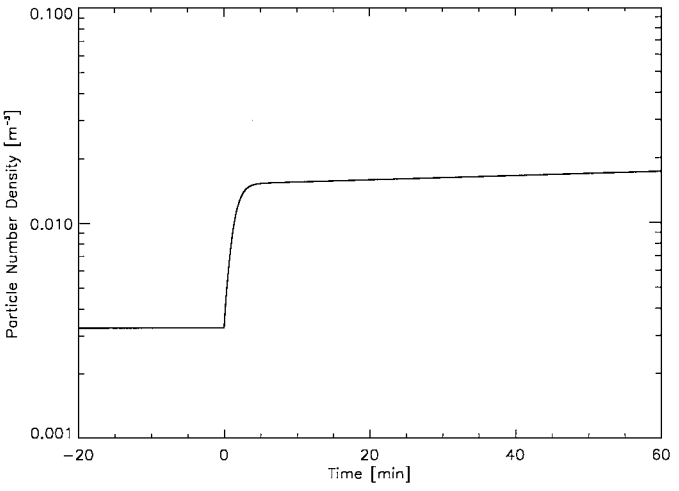

FIG. 7. The number density of chondrule precursors (m^{-3}) as a function of time for the shocked suspension described in the caption to Fig. 6.

a temperature of 1120 K immediately before crossing the shock front. They are then quickly brought to their melting point in under 1 s and achieve a maximum temperature of 1930 K about 1.4 s after passing through the shock front. The chondrules then cool very rapidly over the next 2 min to a temperature of ∼1550 K before reaching a more gradual cooling rate of 20 K h^{-1}, which is consistent with the lower estimates on chondrule cooling rates.

Figure 7 shows the chondrule number density for this simulation (which reaches ∼0.02 m^{-3} downstream of the shock). The chondrules remain above 1500 K for nearly 2.5 h. Using this time and number density in Eq. (1), again keeping $\bar{v} = 100$ cm s^{-1} and $D = 0.1$ cm, to calculate the percentage of chondrules expected to have experienced collisions, the probability is found to be 0.04%. Again, this is two orders of magnitude less than those given by Gooding and Keil (1981). One way of possibly reconciling this is to increase the initial gas density of the nebula (above that expected for a minimum mass nebula) and increase the density of solids proportionally.

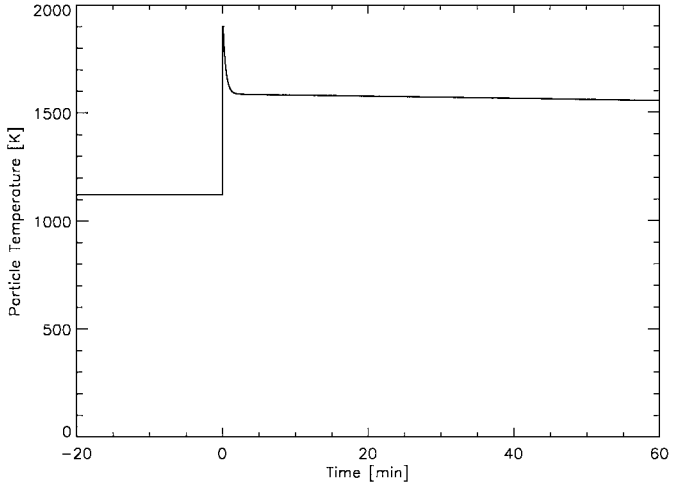

FIG. 6. The temperature of shock-processed chondrule precursors initially suspended at a number density of 0.003 m^{-3} in a nebula with the same gas parameters as the two previous cases studied. The velocity of the shock is 8.2 km s^{-1} with respect to the upstream gas.

5. DISCUSSION

The goal of this paper was to study the formation of chondrules by a shock wave passing through a suspension of particles and nebular gas. To do this, a set of equations that govern the evolution of such a suspension, tracking the dynamical and thermal histories of the chondrules and the gas, was derived and integrated for a variety of conditions. In suspensions such as those studied here, there is a large amount of "feedback" that allows for the chondrules to be processed by the gas and also allows the gas to be affected by the chondrules and their precursors. As the precursors are heated upstream from the shock (for a period of time that depends on the optical depth of the suspension) they will transfer energy to the gas by thermal conduction. Over this period of time, the gas will also be heated and can reach a relatively high temperature compared to its temperature at far distances upstream from the shock. Not only will the temperature change, but because a pressure gradient develops due to the heating, the velocity of the gas with respect to the shock front will change as well. The changes in both of these properties are important in determining the jump conditions across the shock front. This effect is observed in all simulations, the magnitude depending on the density of the particles.

Figure 8 compares the temperature profile of the gas from the simulation done with an initial chondrule density of 0.1 m^{-3}, from Figs. 3 and 4, (solid line) to the profile in the absence of solids, that is, no feedback with the particles (dashed line). Just before the shock front, the gas containing the chondrule precursors reaches a temperature of 785 K, which has a sound speed of 1.95 km s^{-1}, as opposed to 1.39 km s^{-1} at 400 K. The velocity

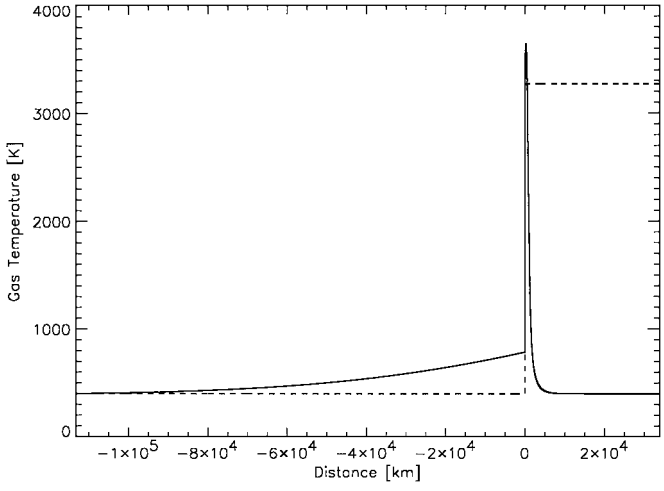

FIG. 8. The temperature profile of nebular gas at a density of 1×10^{-9} g cm^{-3} with a shock moving at a speed of 8.5 km s^{-1} through it. The dashed line is for the case of no particles suspended in the gas; the solid line is for the case of chondrule precursors suspended at a density of 0.1 m^{-3}.

of the gas with respect to the shock front decreased from its initial value by 0.15 km s^{-1} just before the shock. This effectively lowered the shock Mach number from 6.10 to 4.28. The temperature of the gas immediately behind the shock jumped to 3534 K with the chondrule precursors as opposed to 3270 K without them. The chondrules also raise the temperature of the gas downstream from the shock. As the chondrules' velocity decreases, some of their kinetic energy is transferred to the gas as thermal energy. This causes the temperature of the gas to rise to over 100 K higher than what it was immediately behind the shock front.

Figure 9 shows the pressure profiles of the gas in the two cases described for Fig. 8. Not only does the temperature of the gas change because of the presence of solids, but the pressure changes as well. Galy *et al.* (2000) suggested that chondrules formed at high gas pressures. Figure 9 shows that the presence of chondrules in a shocked gas region can aid in achieving those high pressures. The concentration of chondrules will thus help to determine the magnitude of the shock needed to melt chondrules.

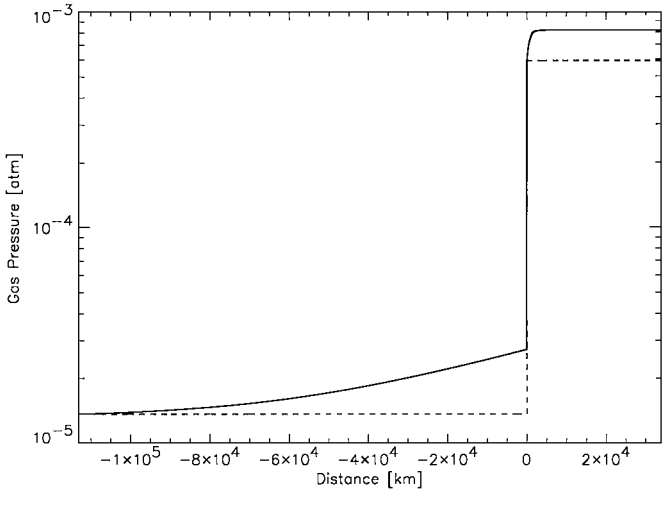

FIG. 9. The pressure profile of the same nebular gas as described in the caption to Fig. 8. The presence of chondrules also causes a higher pressure environment than that predicted given the absence of chondrules.

The cooling rates that the chondrules experienced in our simulation were not constant with time. The experimentally inferred cooling rates of 10–1000 K h^{-1} are based on experiments where melts were cooled linearly, that is, at a constant rate (Hewins 1997). This likely was not the case; because chondrules radiate energy at a rate proportional to T_c^4, all heat sources would have to sum up to the same relationship to prevent the cooling rate from resembling a power law function. Figures 4 and 6 show that chondrules formed in shocks would have cooling rates that varied with time. Figure 6 shows this contrast most dramatically where the chondrules cool about 400 K over a 3-min period, before reaching a much more gradual cooling rate of $\sim$20 K h^{-1}. Similar cooling histories have been tested by Yu and Hewins (1998) and were used to explain retention of Na in type I chondrules. In their experiments, a wide variety of textures was produced that matched well with those of natural chondrules. These textures were dependent on the number of nucleation sites that remained as the samples started to cool, which depends on the peak temperatures reached by the chondrules. Rubin (2000) points out that our understanding of the cooling histories of chondrules is incomplete. Further testing of nonlinear cooling of flash-heated chondrules is needed to understand what cooling histories chondrules could have experienced.

In the cases presented, the cooling rates of the chondrules decreased with lower chondrule precursor number densities. There were two main factors that determined the cooling rates. First, the strongest sources of radiation in the simulation are the hot chondrules immediately behind the shock front. As the chondrules drift away from these radiation sources, the optical depth between them and the hot zone increases. Therefore, the specific intensity of the radiation reaching them decreases as they drift from the shock front. This effect is greater for a higher concentration of particles. Second, the gas behind the shock is constantly transferring heat to the particles either by gas drag or by thermal collisions when the relative velocity is small. When the chondrules gain this energy, they radiate it away, effectively cooling the gas. This effect is also more efficient with a higher concentration of particles. These results may be consistent with the conclusions drawn by Gooding and Keil (1981). Those authors observed that nonporphyritic chondrules experienced more collisions than did porphyritic chondrules. They concluded that nonporphyritic chondrules formed in an environment that had a relatively high concentration of chondrule precursors. Nonporphyritic chondrules experienced much more rapid cooling than did porphyritic chondrules (Radomsky and Hewins 1990). The simulations presented here support the conclusion that those chondrules which cooled more rapidly were formed in zones with high chondrule precursor number

densities. (However, experiments such as those done by Yu and Hewins (1998) suggest that porphyritic chondrules may not have achieved as high a peak temperature or melted as completely as the nonporphyritic chondrules and that the cooling rate played less of a role. Porphyritic chondrules therefore may not have been molten or plastic as long as the nonporphyritic chondrules were and therefore had less time to experience collisions that would have led to cratering or sticking.)

The chondrule precursor density will determine not only the time over which the suspension will cool but also the length of the relaxation zone. This is intuitive, as a given distance from the shock would correspond to a greater optical depth with a higher concentration of chondrules. In the simulation with a chondrule precursor density of 1 m^{-3}, the suspension cooled to its original temperature over a distance of ∼1000 km. Due to the high cooling rates of the chondrules in this simulation, this is unlikely to have been representative of a chondrule forming event. When the precursor density decreased by a factor of 10 and the cooling rates agreed better with experimental estimates, the length of the relaxation zone was ∼15, 000 km. Since this simulation produced chondrules that corresponded to the higher end of the cooling rates, slower cooling rates would require even larger relaxation zones. Therefore, if nebular shocks are responsible for the formation of chondrules, our simulations suggest that they must have been relatively large-scale events in the nebula. Spiral density waves (Wood 1996) or gravitational instabilities (Boss 2000) would be capable of producing shocks of this scale. Smaller scale shocks (e.g., planetesimal bow shocks (Hood 1998) would not produce postshock regions which would allow chondrules to cool at the proper rate under the conditions assumed in this study. These simulations also suggest that if there was a negligible amount of fine-grained dust in the relaxation zone, the initial chondrule precursor densities upstream of the shocks could not have exceeded 0.1 m^{-3}; otherwise we would observe chondrule-type components in meteorites which had cooling rates much greater than 1000 K h^{-1}.

As discussed above and illustrated in Figs. 2, 5, and 7, one of the consequences of a shock wave passing through a particle–gas suspension will be an increase in the density of the resulting chondrules. The ultimate change in density will depend on the velocity of the shock and the initial densities of the precursors and gas. Shock waves themselves may therefore have served as a mechanism for spatially concentrating solids in the nebula. An investigation of how long such concentrations would persist is needed.

While this work has demonstrated the effects on energetics and cooling timescales of the formation of chondrules in a particle–gas suspension, more work is needed to fully evaluate the shock wave mechanism for the formation of chondrules. First, it has been assumed that the suspension extended to infinity regardless of the concentration of chondrules. Obviously, the entire nebula cannot be enriched in solids over solar composition. In fact, Cuzzi *et al*. (2001) showed that higher concentrations of particles occupied smaller volumes in the nebula. While the results presented in this paper show that higher concentrations of chondrules need less spatial distance to be processed, it remains to be investigated how a finite clump of particles is processed in a shock.

In addition, this model has assumed that the hydrogen in the nebula behaved as an ideal gas. Also, radiative cooling due to vibrational and rotational transitions in molecular species has been neglected here. In reality, the dissociation of the hydrogen is likely to be important in determining the temperature profile of the gas in transient heating events such as chondrule formation. These effects have been considered by previous workers (e.g., Iida *et al*. 2001, Desch and Connolly 2002), but they should be reexamined for the case of a particle–gas suspension. As stated above, the gas temperature and density are affected by interactions with the chondrules. This has important effects on the kinetics of the dissociation reaction, for example.

Finally, we have assumed that all solids in our model are present initially as chondrule precursors. This is probably not the case. Some lines of evidence suggest that the chondrule formation environment was enriched in micron-sized dust particles. Specifically, as shown by Liffman and Toscano (2000), this dust may explain the presence of fine-grained mantles around chondrules. Also, the need for high oxygen fugacities (and increases in partial pressures of other mineral-forming elements) can be explained by the vaporization of the dust. The presence of fine-grained dust could have implications for cooling rates of chondrules and the distances in the nebula needed for processing. Sahagian and Hewins (1992) showed that fine-grained dust could help to decrease the spatial scale of the chondrule-forming zone. For this reason, small-scale shocks such as planetesimal bow shocks cannot be completely dismissed (Hood and Ciesla 2001). Incorporation of a fine-dust component into the particle–gas suspension is an important consideration for future work.

Shock waves continue to be viable mechanisms for chondrule formation. The exact source of the shocks still needs to be determined. The simulations presented here demonstrate that large shocks are capable of producing chondrules that would have cooled in a manner consistent with the experimentally derived rates, though these rates need to be revisited due to the nonlinear cooling that chondrules would have experienced in these events. Shocks from gravitational instabilities or spiral density waves are the leading mechanisms to produce these shocks.

APPENDIX: DERIVATION OF MULTIPARTICLE EQUATIONS

The equations describing gas–particle energy and momentum transfer behind the shock front for a single particle are (Hood and Horanyi 1991)

$$m_c C_c \frac{dT_c}{dt} = \pi D^2 q_d + \frac{\pi}{4} D^2 \varepsilon_{abs} J_r - \pi D^2 \varepsilon_{emc} \sigma T_d^4 \quad \text{(A1)}$$

$$m_c \frac{dV_a}{dt} = -\pi D^2 \frac{C_D}{8} \rho_g V_a |V_a|, \quad \text{(A2)}$$

where the only changes in notation are that ρ_g replaces ρ as the mass density of the gas, the particle diameter is used instead of the radius, and the subscript c now denotes chondrule. Here V_a represents the velocity of the chondrule with respect to the gas (note that this is written slightly differently than in HH91 so as to assign a direction to the velocity).

We are interested in how the properties of both the gas and chondrules change behind the shock. Because the two phases travel at different velocities through the relaxation zone, we shall consider how they change with distance behind the shock rather than as a function of time. To make this change, we use the chain rule:

$$\frac{d}{dx} = \frac{dt}{dx}\frac{d}{dt} \tag{A3}$$

$$v_c = \frac{dx}{dt} \tag{A4}$$

$$\frac{d}{dx} = \frac{1}{v_c}\frac{d}{dt} \tag{A5}$$

$$v_c\frac{d}{dx} = \frac{d}{dt}. \tag{A6}$$

Using this relation, the initial equations become:

$$m_c v_c C_c \frac{dT_c}{dx} = \pi D^2 q_d v_c + \frac{\pi}{4} D^2 v_c \varepsilon_{abs} J_r - \pi D^2 v_c \varepsilon_{emc} \sigma T_d^4 \tag{A7}$$

$$m_c v_c \frac{dV_a}{dt} = -\pi D^2 v_c \frac{C_D}{8} \rho_g V_a |V_a|. \tag{A8}$$

If we assign to the gas a temperature T_g and a velocity v_g, the momentum equation then becomes:

$$m_c v_c \frac{d(v_c - v_g)}{dx} = -\pi D^2 v_c \frac{C_d}{8} \rho_g (v_c - v_g)|v_c - v_g|. \tag{A9}$$

One of the fundamental assumptions of the single particle case is that the gas properties behind the shock do not change. If that is the case, then the velocity of the gas remains constant and the momentum equation reduces to:

$$m_c v_c \frac{dv_c}{dx} = -\pi D^2 v_c \frac{C_d}{8} \rho_g (v_c - v_g)|v_c - v_g|. \tag{A10}$$

This gives the momentum of the chondrule with respect to the shock front, whereas the HH91 equation considers the momentum with respect to the gas.

As mentioned, these equations are for a single particle, whereas we are interested in a suspension filled with chondrules. Therefore, we must consider equations which describe the change in terms of the number of chondrules in a given volume. A general procedure to do this is to multiply by the number of chondrules per unit volume:

$$\frac{equation}{particle} \times \frac{particles}{cm^3} = \frac{equation}{cm^3}. \tag{A11}$$

This allows us to rewrite the equations describing the change in energy and momentum of the chondrules as:

$$m_c v_c n_c C_c \frac{dT_c}{dx} = \pi v_c n_c D^2 q_d + \frac{\pi}{4} D^2 v_c n_c \varepsilon_{abs} J_r - \pi D^2 v_c n_c \varepsilon_{emc} \sigma T_d^4 \tag{A12}$$

$$m_c v_c n_c \frac{dv_c}{dx} = -\pi D^2 v_c n_c \frac{C_d}{8} \rho_g (v_c - v_g)|v_c - v_g|. \tag{A13}$$

The right-hand side of (A13) can be recognized as our expression for F_D in the description of our model, allowing us to write the momentum equation as

$$\rho_c v_c \frac{dv_c}{dx} = F_D, \tag{A14}$$

where we have substituted ρ_c for the product $m_c n_c$. With use of the mass continuity equation,

$$\frac{d}{dx}(\rho_c v_c) = 0, \tag{A15}$$

we finally get

$$\frac{d}{dx}\left(\rho_c v_c^2\right) = F_D. \tag{A16}$$

In the energy equation (A12), we can identify the first term on the right as the rate at which energy is transferred from the gas to the chondrules due to gas drag and thermal collisions. The second term is the rate at which chondrules absorb radiation from the radiation field they are immersed in, and the third is the rate at which the chondrules lose energy through radiation. In the text of the paper, we identified these terms as Q_{gc}, Q_{cc}, and Q_{cr}, and they are found by the method described in this paper and in HH91.

Equation (A12) describes how the internal energy of the chondrules changes with distance behind the shock. However, we are concerned with how the total energy of the chondrules changes, and thus we must consider the kinetic energy of the particles as well. The change in kinetic energy of the chondrules is controlled by the forces acting on them: in this case there is only the drag force exerted by the gas. For a single particle,

$$\Delta E_{kinetic} = \int F_d \, dx, \tag{A17}$$

where F_d is the drag force exerted on a single chondrule (F_D/n_c). This means

$$\frac{dE_{kinetic}}{dx} = F_d \tag{A18}$$

$$\frac{d}{dx}\left(\frac{1}{2} m_c v_c^2\right) = F_d. \tag{A19}$$

Since we are considering a suspension and not just a single particle, we multiply by n_c to get

$$m_c n_c \frac{d}{dx}\left(\frac{1}{2} v_c^2\right) = n_c F_d, \tag{A20}$$

where we have moved m_c outside the derivative because it is a constant. We can rewrite this equation as

$$\rho_c \frac{d}{dx}\left(\frac{1}{2} v_c^2\right) = F_D. \tag{A21}$$

To get the *rate* of kinetic energy transfer per unit volume, we multiply by the velocity v_c to get

$$\rho_c v_c \frac{d}{dx}\left(\frac{1}{2} v_c^2\right) = F_D v_c. \tag{A22}$$

Adding this to (A12), and using the mass continuity equation again, we finally get

$$\frac{d}{dx}\left[\left(C_c T_c + \frac{1}{2} v_c^2\right)\rho_c v_c\right] = Q_{gc} + Q_{cc} - Q_{cr} + F_D v_c. \tag{A23}$$

As for the equations describing the evolution of the gas behind the shock, it too obeys the mass continuity equation:

$$\frac{d}{dx}(\rho_g v_g) = 0. \tag{A24}$$

The momentum of the gas is given by $\rho_g v_g^2 + P$. The only source or sink of momentum from the gas is the chondrules, and it will be opposite in sign to the change in momentum of the chondrules. Thus,

$$\frac{d}{dx}\left(\rho_g v_g^2 + P\right) = -F_D. \tag{A25}$$

Likewise, the loss or gain in energy for the gas is controlled by the chondrules. Again, what is a source for the chondrules will be a sink for the gas and vice versa. Thus, the transfer terms for the gas will be equal and opposite to those of the chondrules. The energy flux density of the gas is given by $\rho_g(w + \frac{1}{2}v_g^2)$, where w is the specific enthalpy of the gas, which can be rewritten as $C_v T_g + P$. Thus, the rate of energy change per unit volume of the gas is

$$\frac{d}{dx}\left[\left(C_v T_g + \frac{1}{2}v_g^2\right)\rho_g v_g + P v_g\right] = -Q_{gc} - F_D v_c. \tag{A26}$$

ACKNOWLEDGMENTS

This work was supported by a grant from NASA's Origins program. We thank David Kring for useful discussions relating to the interpretation of meteoritic data. We are also grateful to Dante Lauretta for helpful discussions about meteoritic data and for providing suggestions on improvements to the manuscript. We also thank Steve Desch for reviews of earlier versions of this manuscript and suggestions on how to treat the radiative transfer. An anonymous reviewer provided detailed comments and criticisms that resulted in significant improvements to the paper.

REFERENCES

Boss, A. P. 1996. A concise guide to chondrule formation models. In *Chondrules and the Protoplanetary Disk* (R. H. Hewins, R. H. Jones, and E. R. D. Scott, Eds.), pp. 257–263. Cambridge Univ. Press, Cambridge, UK.

Boss, A. P. 2000. Possible rapid gas giant planet formation in the solar nebula and other protoplanetary disks. *Astrophys. J.* **53**, L101–104.

Ciesla, F. J., and L. L. Hood 2000. Chondrule formation in nebular shocks: An improved one-dimensional model. *Lunar Planet. Sci.* **31**, 1650 (abstract).

Collison, A. J., and J. D. Fix 1991. Axisymmetric models of circumstellar dust shells. *Astrophys. J.* **368**, 545–557.

Connolly, H. C., and S. G. Love 1998. The formation of chondrules: Petrologic tests of the shock wave model. *Science* **280**, 62–67.

Cuzzi, J. N., A. R. Dobrovolskis, and R. C. Hogan 1996. Turbulence, chondrules, and planetesimals. In *Chondrules and the Protoplanetary Disk* (R. H. Hewins, R. H. Jones, and E. R. D. Scott, Eds.), pp. 35–44. Cambridge Univ. Press, Cambridge, UK.

Cuzzi, J. N., R. C. Hogan, J. M. Paque, and A. R. Dobrovolskis 2001. Size-selective concentration of chondrules and other small particles in protoplanetary nebula turbulence. *Astrophys. J.* **546**, 496–508.

Desch, S. J., and H. C. Connolly 2002. A model of the thermal processing of particles in solar nebula shocks: Application to the cooling rates of chondrules. *Meteoritics* **37**, 183–207.

Galy, A., E. D. Young, R. D. Ash, and R. K. O'Nions 2000. The formation of chondrules at high gas pressures in the solar nebula. *Science* **290**, 1751–1754.

Gombosi, T. I., A. F. Nagy, and T. E. Cravens 1986. Dust and neutral gas modeling of the inner atmospheres of comets. *Rev. Geophys.* **24**, 667–700.

Gooding, J. L., and K. Keil 1981. Relative abundances of chondrule primary textural types in ordinary chondrites and their bearing on conditions of chondrule formation. *Meteoritics* **16**, 17–43.

Hewins, R. H. 1997. Chondrules. *Annu. Rev. Earth Planet. Sci.* **25**, 61–83.

Hood, L. L. 1998. Thermal processing of chondrule precursors in planetesimal bow shocks. *Meteoritics* **33**, 97–107.

Hood, L. L., and F. J. Ciesla 2001. The scale size of chondrule formation regions: Constraints imposed by chondrule cooling rates. *Meteoritics* **36**, 1571–1585.

Hood, L. L., and M. Horanyi 1991. Gas dynamic heating of chondrule precursor grains in the solar nebula. *Icarus* **93**, 259–269.

Hood, L. L., and M. Horanyi 1993. The nebular shock wave model for chondrule formation: One-dimensional calculations. *Icarus* **106**, 179–189.

Hood, L. L., and D. A. Kring 1996. Models for multiple heating mechanisms. In *Chondrules and the Protoplanetary Disk* (R. H. Hewins, R. H. Jones, and E. R. D. Scott, Eds.), pp. 257–263. Cambridge Univ. Press, Cambridge, UK.

Huang, S., J. Lu, M. Prinz, M. K. Weisberg, P. H. Benoit, and D. G. Sears 1996. Chondrules: Their diversity and the role of open-system processes during their formation. *Icarus* **122**, 316–346.

Igra, O., and G. Ben-Dor 1980. Parameters affecting the relaxation zone behind normal shock waves in a dusty gas. *Isr. J. Tech.* **18**, 159–168.

Iida, A., T. Nakamoto, H. Susa, and Y. Nakagawa 2001. A shock heating model for chondrule formation in a protoplanetary disk. *Icarus* **153**, 430–450.

Kring, D. A. 1988. *The Petrology of Meteoritic Chrondrules: Evidence for Fluctuating Conditions in the Solar Nebula*. Ph.D. thesis, Harvard University, Cambridge, MA.

Kring, D. A. 1991. High temperature rims around chondrules in primitive chondrites: Evidence for fluctuating conditions in the solar nebula. *Earth Planet. Sci. Lett.* **105**, 65–80.

Landau, L. D., and E. M. Lifshitz 1959. *Fluid Mechanics*. Pergamon, Elmsford, New York.

Lauretta, D. S., P. R. Buseck, and T. J. Zega 2001. Opaque minerals in the matrix of the Bishunpur (LL3.1) chondrite: Constraints on the chondrule formation environment. *Geochim. Cosmochim. Acta* **65**, 1337–1353.

Liffman, K., and M. Toscano 2000. Chondrule fine-grained mantle formation by hypervelocity impact of chondrules with a dusty gas. *Icarus* **143**, 106–125.

Lofgren, G. E., and B. Hanson 1997. Formation of compound chondrules by low-velocity collisions. *Meteoritics* **32**, A81.

Mihalas, D. 1970. *Stellar Atmospheres*. Freeman, San Francisco.

Ozawa, K., and H. Nagahara 1997. Stability of chondrule melt in the solar nebula. *Lunar Planet. Sci.* **28**, (abstract).

Ozisik, M. N. 1977. *Basic Heat Transfer*. Mc-Graw–Hill, New York.

Radomsky, P. M., and R. H. Hewins 1990. Formation conditions of pyroxene–olivine and magnesian olivine chondrules. *Geochim. Cosmochim. Acta* **54**, 3475–3490.

Rubin, A. E. 2000. Petrologic, geochemical and experimental constraints on models of chondrule formation. *Earth Sci. Rev.* **50**, 3–27.

Ruzmaikina, T. V., and W. H. Ip 1994. Chondrule formation in radiative shock. *Icarus* **112**, 430–447.

Sahagian, D. L., and R. H. Hewins 1992. The size of chondrule-forming events. *Lunar Planet. Sci.* **23**, 1197 (abstract).

Tanaka, K. K., H. Tanaka, K. Nakazawa, and Y. Nakagawa 1998. Shock heating due to accretion of a clumpy cloud onto a protoplanetary disk. *Icarus* **134**, 137–154.

Wasson, J. T., A. N. Krot, S. L. Min, and A. E. Rubin 1995. Compound chondrules. *Geochim. Cosmochim. Acta* **59**, 1847–1869.

Weidenschilling, S. J. 1984. Evolution of grains in a turbulent solar nebula. *Icarus* **60**, 553–567.

Weidenschilling, S. J. 1988. Formation processes and time scales for meteorite parent bodies. In *Meteorites and the Early Solar System* (J. F. Kerridge and M. S. Matthews, Eds.), pp. 680–696. Univ. of Arizona Press, Tucson.

Weidenschilling, S. J., F. Mazari, and L. L. Hood 1998. The origin of chondrules at jovian resonances. *Science* **279**, 681–684.

Whipple, F. L. 1950. Theory of micro-meteorites. I. In an isothermal atmosphere. *Proc. Natl. Acad. Sci. USA* **86**, 687–695.

Wood, J. A. 1984. On the formation of meteoritic chondrules by aerodynamic drag heating in the solar nebula. *Earth Planet Sci. Lett.* **70**, 11–26.

Wood, J. A. 1985. Meteoritic constraints on processes in the solar nebula. In *Protostars and Planets II* (D. C. Black and M. S. Matthews, Eds.), pp. 687–702. Univ. of Arizona Press, Tucson.

Wood, J. A. 1996. Processing of chondritic and planetary material in spiral density waves in the nebula. *Meteoritics Planet. Sci.* **31**, 641–645.

Yu, Y., and R. Hewins 1998. Transient heating and chondrule formation: Evidence from sodium loss in flash heating simulation experiments. *Geochim. Cosmochim. Acta* **62**, 159–172.